Electronic Supplementary Material (ESI) for Chemical Communications.
This journal is © The Royal Society of Chemistry and the Centre National de la Recherche Scientifique 2020

An Ionic Liquid-Modified RGO/Polyaniline Composite for High-Performance Flexible All-Solid-State Supercapacitors

Chang Dong, Xiaoling Zhang, Yijia Yu, Liyan Huang*, Jun Li, Ying Wu and Zhengping Liu

Address: Beijing Key Laboratory of Energy Conversion and Storage Materials, College of Chemistry, Beijing Normal University, Beijing 100875, P. R. China

E-mail: hly@bnu.edu.cn

Experimental

Materials

All chemical agents were of analytical grade. The 1,3-propionic sulfonate, *N*-methyl-imidazole, aniline (ANI), graphene oxide (GO), sulfuric acid (H_2SO_4), carbon black (Alfa-Aesar), hydrochloric acid (HCl), ethanol and ammonium sulfate (APS) were obtained from Shanghai Aladdin Co. Polyvinylidine fluoride (PVDF) and *N*-methyl-2-pyrrolidone (NMP) were purchased from Shanghai Chemical Reagent Co. *N*-methyl-imidazole and ANI were distilled under reduced pressure before use.

Preparation of RGO-IL/PANI

The RGO-IL was prepared by a hydrothermal method. 1-(3-sulfonic acid) propyl-3-methylimidazolium hydrogen sulfate ([PSMIM][HSO_4]) was synthesized by referenced methods[1]. A 30 mL GO dispersion (3 mg mL^{-1}) was mixed with [PSMIM][HSO_4] in a round-bottomed flask (50 mL). After homogenization by sonication, the mixture was transferred to a reaction kettle and maintained at 180 °C for 20 h. The obtained composite was rinsed with water for three times and freeze-dried overnight.

The RGO-IL/PANI was synthesized as follows. The RGO-IL (10 mg) and ANI (80 mg) were dispersed in a water/ethanol mixture (v:v = 7:3) and then stirred at 300 rpm at 0-5 °C for 3 h. Subsequently, the pH of the mixture was adjusted to 1.5 with 1 M HCl, and APS solution with an equal molar amount of ANI was added dropwise to the mixture. The polymerization was held at 0-5 °C for 24 h. Finally, the resultant product was washed with water and ethanol and then dried at 60 °C in a vacuum oven to obtain RGO-IL/PANI. For comparison, the same procedure was conducted for unmodified RGO, and the resulting sample was named RGO/PANI.

Preparation of the Working Electrodes

A mixture of RGO-IL/PANI, carbon black and PVDF in NMP solvent was uniformly mixed at a mass ratio of 85:10:5 and coated on a stainless steel wire mesh substrate. After drying, the working electrode was ready for use.

Structural Characterization

Fourier transform infrared (FTIR) spectroscopy of the samples was conducted in the range of 500-4000 cm^{-1} using a FTIR spectrometer (IRAffinity-1, Shimadzu, Japan). The weight loss of the samples was obtained by thermogravimetric analysis (TGA, Mettler Toledo TGA2) at a heating rate of 10 °C min^{-1} between 25 and 600 °C under the protection of nitrogen. X-ray powder diffraction (XRD) patterns were recorded by using a diffractometer (Ultima, MiniFlex 600). X-ray photoelectron spectroscopy analyses (XPS, Thermofisher, ESCALAB 250Xi) were performed to probe the elemental and bond components. Scanning electron microscopy (SEM, Hitachi SU8010) was performed to analyse the surface morphology of the samples. The specific surface area and pore size distribution were determined by nitrogen adsorption-desorption method (Quantachrom, Autosorb-iQ).

Electrochemical Characterization

In this study, the electrochemical properties of the electrodes were analysed with cyclic voltammetry (CV), galvanostatic charge/discharge (GCD) and electrochemical impedance spectroscopy (EIS) measurements based on a three-electrode system and two-electrode system (coin-type supercapacitor device and flexible all-solid-state supercapacitor device). Herein, CV, GCD and EIS tests were conducted on an electrochemical workstation (CHI660E, Chenhua).

For the three-electrode system, RGO-IL/PAN was used as the working electrode. In addition, a Pt plate, a SCE and 1 M H_2SO_4 were used as the counter electrode, the reference electrode and the electrolyte, respectively. For the two-electrode system, the coin-type supercapacitor was assembled by using two identical electrodes that were cut into circles with a diameter of 1 cm, and a glass fibre cloth acted as the separator. To construct the flexible all-solid-state supercapacitor device, two prepared working electrodes were sandwiched with the PVA-H_2SO_4 gel electrolyte and dried at 60 °C.

In the three-electrode system, the gravimetric specific capacitance C_s (F g^{-1}) was calculated according to $C_s=I\Delta t/(m\Delta V)$, where I is the discharge current (A), ΔV is the working voltage window and m is the active substance weight (g) of the working electrode. In the two-electrode cell system, C_s (F g^{-1}) was calculated according to $C_s=4I\Delta t/(m\Delta V)$, where I, ΔV and m represent the same as above. The discharge energy density E_{cell} (Wh kg^{-1}) was calculated by $E_{cell}=C_sV^2/8$. The power density P_{cell} (W kg^{-1}) was calculated by $P_{cell}=E_{cell}/t$, where t means the discharge time.

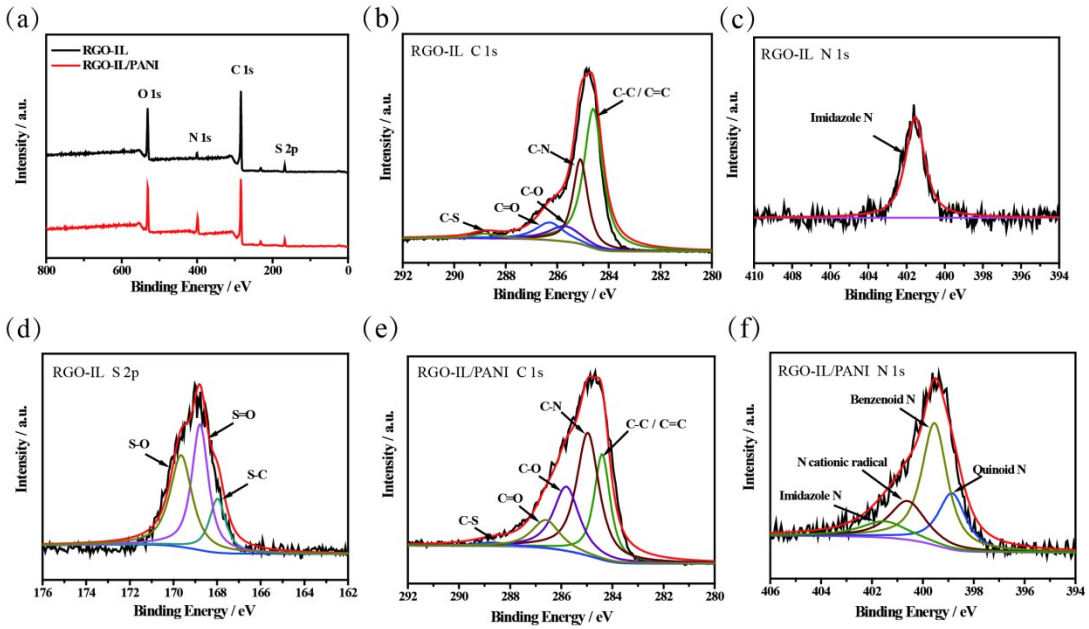

Fig. S1 XPS spectra of RGO-IL and RGO-IL/PANI: (a) survey spectra. (b) C 1s, (c) N 1s and (d) S 2p spectrum of RGO-IL. (e) C 1s and (f) N 1s spectrum of RGO-IL/PANI.

The elemental and bond components for RGO-IL and RGO-IL/PANI were further characterized by X-ray photoelectron spectroscopy (XPS). As shown in Fig. S1a, both RGO-IL and RGO-IL/PANI presented four peaks at 168.2, 284.8, 399.8, and 531.7 eV, confirming the presence of S, C, N, and O, respectively. It was clear that the S element was derived from the sulfonate groups in IL, indicating the successful modification of IL. We suggested that the N element of RGO-IL was mainly from the imidazole ring nitrogen in IL, while the N element of RGO-IL/PANI was from IL and PANI, so that the intensity of RGO-IL/PANI was increased significantly compared with that of RGO-IL. The C 1s peak of RGO-IL (Fig. S1b) contained five components. The subpeaks at 284.4 eV, 284.9 eV, 285.7, 286.6 and 288.8 eV were attributed to C-C/C=C, C-N, C-O, C=O and C-S[2, 3], respectively. The N 1s peak of RGO-IL (Fig. S1c) was corresponded to the imidazole ring nitrogen, confirming the presence of IL. It was further confirmed by the S 2p peak (Fig. S1d), which was divided into S-C (167.9 eV), S=O (168.7 eV) and S-O (169.6 eV) bonds[3], respectively, indicating the presence of the sulfonate groups from IL. The C 1s peak of RGO-IL/PANI (Fig. S1e) was deconvoluted into five subpeaks at 284.4, 284.9, 285.7, 286.6 and 288.8 eV, which were attributed to C-C/C=C, C-N, C-O, C=O and C-S, respectively. Compared with RGO-IL, the peak density of C-N in RGO-IL/PANI was greatly increased, revealing the successful coating of PANI. Similarly, due to the formation of PANI, the N 1s peak of RGO-IL/PANI (Fig. S1f) was resolved into four subpeaks at 398.8, 399.5, 400.6 and 401.5 eV, corresponding to the quinoid amine, the benzenoid amine, the nitrogen cationic radical and the imidazole ring nitrogen[4, 5], respectively. The above characterization confirmed the successful preparation of RGO-IL/PANI.

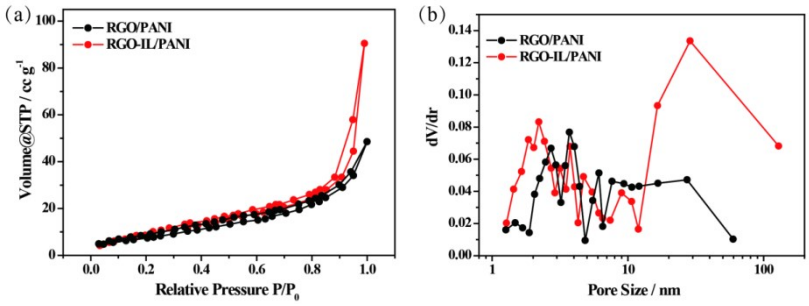

Fig. S2 (a) Nitrogen adsorption isotherms of RGO/PANI and RGO-IL/PANI. (b) BJH desorption pore size distribution curves of RGO/PANI and RGO-IL/PANI.

The specific surface area and pore size distribution of RGO/PANI and RGO-IL/PANI were also investigated by N_2 adsorption-desorption testing. As shown in Fig. S2, both samples exhibited typical type IV isotherm curves, demonstrating the existence of a mesoporous structure. The pore size distribution revealed that RGO-IL/PANI possessed a wider mesopore diameter than RGO/PANI, which could increase the contact between the electrode with the electrolyte. The surface areas were calculated on the basis of the BET method. The specific surface areas of the RGO/PANI and RGO-IL/PANI were 48.43 and 85.12 m^2 g^{-1}, respectively. The large specific surface areas increased the space for store charge in the electrode.

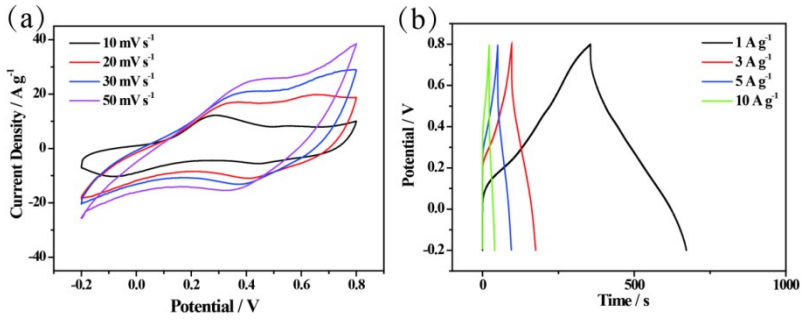

Fig. S3 (a) CV curves of RGO/PANI at different scanning rates. (b) GCD curves of RGO/PANI at current densities from 1 to 10 A g^{-1}.

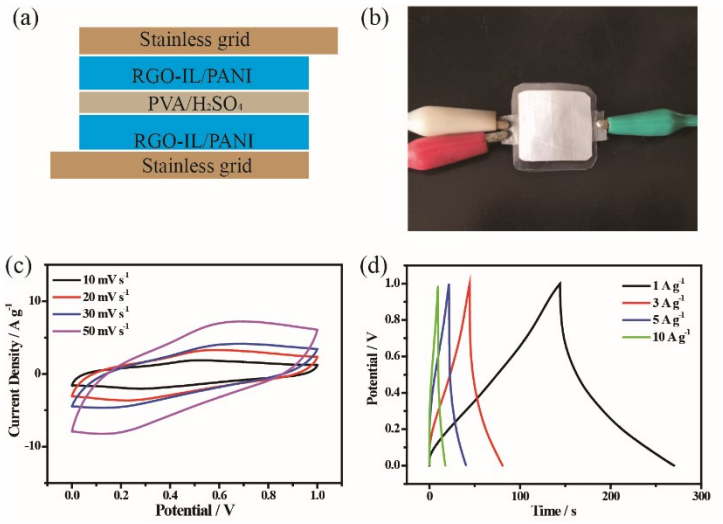

Fig. S4 (a) Schematic presentation of the flexible all-solid-state supercapacitor. (b) Photographs of the assembled flexible all-solid-state supercapacitor. (c) CV curves of RGO-IL/PANI based flexible all-solid-state supercapacitor at different scanning rates. (d) GCD curves of RGO-IL/PANI based flexible all-solid-state supercapacitor at current densities from 1 to 10 A g^{-1}.

Finally, we used the solid electrolyte instead of the liquid electrolyte to fabricate a flexible all-solid-state supercapacitor device (Fig. S4a and b) and measured the capacitive nature of the RGO-IL/PANI composite. As shown in Fig. S4c, the CV curves retained similar shapes at different scan rates without significant changes in the redox peaks, demonstrating good electrochemical stabilities. The GCD curves at different current densities are shown in Fig. S4d, and the specific capacitances were 508, 432, 385 and 320 F g^{-1} at current densities of 1, 3, 5, and 10 A g^{-1} , respectively. The device maintained 63% of its capacitance when the current density was increased to 10 times the initial density, indicating excellent capacitance performance and a high rate performance.

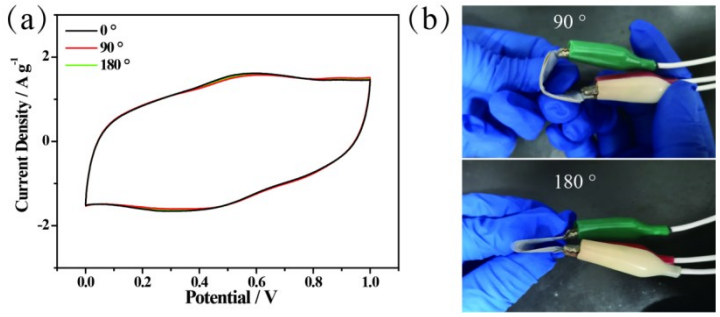

Fig. S5 (a) CV curves of the flexible all-solid-state device at a scan rate of 10 mV s^{-1} under 0 °, 90 ° and 180 ° bending states. (b) 90 ° and 180 ° bending states of the flexible all-solid-state device.

To examine the flexibility of the device, the electrochemical performance was tested under different bending conditions. As shown in Fig. S5, no significant changes could be seen in the CV curves of the RGO-IL/PANI supercapacitor device under bending conditions of 90 and 180 degrees, indicating the excellent flexibility of RGO-IL/PANI and potential as a flexible electrode for high performance supercapacitors.

References

1 G. Zhao, T. Jiang, H. Gao, B. Han, J. Huang, D. Sun, *Green Chem.,* 2004, **6**, 75.
2 K. Chi, Z.Y. Zhang, J.B. Xi, Y.G. Huang, F. Xiao, S. Wang, Y.Q. Liu, *ACS Appl. Mater. Inter.*, 2014, **6**, 16312.
3 H. Yu, G. Xin, X. Ge, C. Bulin, R. Li, R. Xing, B. Zhang, *Compos. Sci. Technol.,* 2018, **154**, 76.
4 K. Zhang, L. Zhang, X.S. Zhao, J. Wu, *Chem. Mater.*, 2010, **22**, 1392.
5 P. Bhunia, E. Hwang, M. Min, J. Lee, S. Seo, S. Some, H. Lee, *Chem. Commun.*, 2012, **48**, 913.